

# Impact of $\pi N \rightarrow \pi\pi N$ data on determining high-mass nucleon resonances

Hiroyuki Kamano

*Research Center for Nuclear Physics,  
Osaka University, Ibaraki, Osaka 567-0047, Japan*

## Abstract

Motivated by an experimental proposal for the measurement of the  $\pi N \rightarrow \pi\pi N$  reactions at J-PARC, we examine the potential impact of the  $\pi N \rightarrow \pi\pi N$  cross section data on the determination of the resonance parameters of the high-mass  $N^*$  states. For this purpose, we make use of the ANL-Osaka dynamical coupled-channels model, which has been developed recently through a combined analysis of the unpolarized cross section as well as polarized observables from pion- and photon-induced  $\pi N$ ,  $\eta N$ ,  $K\Lambda$ , and  $K\Sigma$  production reactions off a proton target. We present predictions for the  $\pi N \rightarrow \pi\pi N$  total cross sections and invariant mass distributions, and demonstrate that the  $\pi N \rightarrow \pi\pi N$  differential cross section data can indeed be a crucial source of information for understanding  $N^* \rightarrow \pi\Delta$ ,  $\rho N$ ,  $\sigma N \rightarrow \pi\pi N$  decay of the high-mass  $N^*$  states.

PACS numbers: 14.20.Gk, 13.75.Gx, 13.60.Le

## I. INTRODUCTION

Most of the high-mass nucleon resonances ( $N^*$ ), of which complex pole mass  $M_R$  satisfies  $\text{Re}(M_R) \gtrsim 1.6$  GeV, are known to decay strongly to the three-body  $\pi\pi N$  continuum states. Furthermore, it is also known that the double-pion production processes dominate the cross sections of  $\pi N$  and  $\gamma N$  reactions above  $W \sim 1.6$  GeV. These facts naturally lead to the realization that the reaction analyses including double-pion production data are indispensable to establishing the mass spectrum of the high-mass  $N^*$  states, which remains poorly understood despite years of study.

Such analyses, however, are not easy to pursue at the present time mainly due to the lack of the data of  $\pi N \rightarrow \pi\pi N$  in the relevant energy region above  $W \sim 1.6$  GeV. In fact, in this energy region practically no differential cross section data of  $\pi N \rightarrow \pi\pi N$  are available for detailed partial wave analyses. (See, e.g., Refs. [1–4] for the details of the current situation of the world data of  $\pi N \rightarrow \pi\pi N$ .) Although the high statistics data of  $\gamma N \rightarrow \pi\pi N$  are becoming available from electron/photon beam facilities such as JLab, Bonn, Mainz, SPring-8, and ELPH at Tohoku University, the  $\pi N \rightarrow \pi\pi N$  data are still highly desirable because it is free from electromagnetic interactions of hadrons that bring additional complications to the analyses.

It is therefore quite encouraging to see the approval of an experimental proposal at J-PARC to develop plans for performing precise measurements of  $\pi^\pm p \rightarrow \pi\pi N$  above  $W \sim 1.6$  GeV (J-PARC E45 [5]). Once such precise data are available and included in partial wave analyses, the current  $N^*$  mass spectrum might require significant modifications. Besides this, understanding of the final state interactions of the three-body  $\pi\pi N$  state is also very important for constructing neutrino-induced reaction models in the GeV-energy region. A precise knowledge of neutrino-nucleon/nucleus interactions is required for the determination of leptonic  $CP$  phase and the neutrino mass hierarchy through accelerator and atmospheric neutrino experiments (see, e.g., Refs. [6, 7]).

In this work, we examine whether the  $\pi N \rightarrow \pi\pi N$  data can provide crucial constraints on the determination of the  $N^*$  resonance parameters such as pole positions and decay branching ratios. For this purpose, we make use of a reaction model recently described in Ref. [8], which is based on the ANL-Osaka dynamical coupled-channels (DCC) approach [9]. In this approach, the amplitudes of meson production reactions off a nucleon are given by solving the unitary coupled-channels integral equations. As a result, it is ensured that the amplitudes satisfy the two- and three-body unitarity. In the DCC model of Ref. [8], the  $\pi N$ ,  $\eta N$ ,  $\pi\pi N$  ( $\pi\Delta$ ,  $\rho N$ ,  $\sigma N$ ),  $K\Lambda$ , and  $K\Sigma$  channels are taken into account and the model parameters are determined by a comprehensive analysis of both pion- and photon-induced  $\pi N$ ,  $\eta N$ ,  $K\Lambda$ , and  $K\Sigma$  production reactions off a proton target, where the data up to  $W = 2.3$  GeV are taken into account for  $\pi N \rightarrow \pi N$  and those up to  $W = 2.1$  GeV are for the other reactions.

## II. ANL-OSAKA DCC MODEL FOR THE $\pi N \rightarrow \pi\pi N$ REACTION

In the ANL-Osaka DCC approach [2, 9], the  $\pi N \rightarrow \pi\pi N$  amplitude has the graphical representation shown in Fig. 1 and is written explicitly as,

$$T_{\pi\pi N, \pi N} = T_{\pi\pi N, \pi N}^{\text{dir}} + \sum_{MB=\pi\Delta, \sigma N, \rho N} T_{\pi\pi N, \pi N}^{MB}, \quad (1)$$

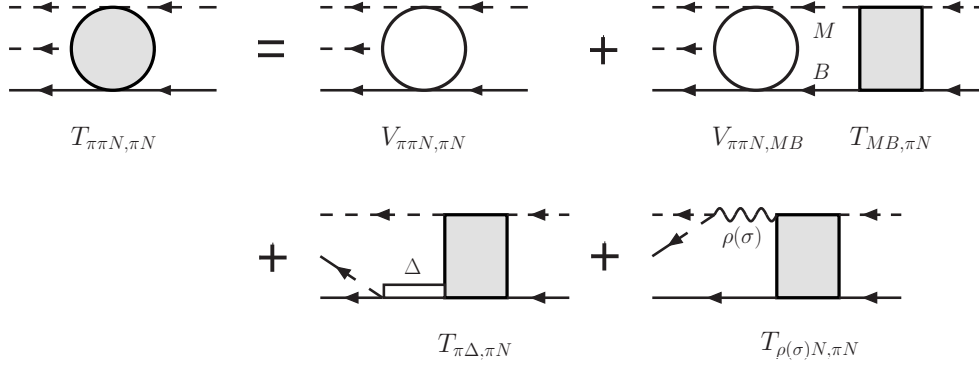


FIG. 1. Graphical representation of Eq. (1).

with

$$T_{\pi\pi N, \pi N}^{\text{dir}} = V_{\pi\pi N, \pi N} + \sum_{MB} V_{\pi\pi N, MB} G_{MB} T_{MB, \pi N}, \quad (2)$$

$$T_{\pi\pi N, \pi N}^{\pi\Delta} = \Gamma_{\pi N, \Delta} G_{\pi\Delta} T_{\pi\Delta, \pi N}, \quad (3)$$

$$T_{\pi\pi N, \pi N}^{\rho N} = \Gamma_{\pi\pi, \rho} G_{\rho N} T_{\rho N, \pi N}, \quad (4)$$

$$T_{\pi\pi N, \pi N}^{\sigma N} = \Gamma_{\pi\pi, \sigma} G_{\sigma N} T_{\sigma N, \pi N}. \quad (5)$$

Here  $V_{\pi\pi N, MB}$  is a potential describing the direct two-body to three-body transition processes [2];  $G_{MB}$  is the Green's function of the  $MB$  channel;  $\Gamma_{\pi N, \Delta}$ ,  $\Gamma_{\pi\pi, \rho}$ , and  $\Gamma_{\pi\pi, \sigma}$  are the decay vertices for  $\Delta \rightarrow \pi N$ ,  $\rho \rightarrow \pi\pi$ , and  $\sigma \rightarrow \pi\pi$ , respectively. The summation  $\sum_{MB}$  in Eq. (2) runs over  $MB = \pi N, \eta N, \pi\Delta, \rho N, \sigma N, K\Lambda, K\Sigma$ . As for the two-body amplitudes  $T_{MB, \pi N}$ , we employ those obtained in our recent DCC analysis [8], which is completely unitary in the  $\pi N$ ,  $\eta N$ ,  $\pi\pi N(\pi\Delta, \rho N, \sigma N)$ ,  $K\Lambda$ , and  $K\Sigma$  channel space. The detailed description of the two-body amplitudes, meson-baryon Green's functions, and decay vertices in the above equations can be found in Ref. [8] and will not be presented here.

### III. PREDICTED TOTAL CROSS SECTIONS OF THE $\pi N \rightarrow \pi\pi N$ REACTION

Figure 2 shows the  $\pi N \rightarrow \pi\pi N$  total cross sections up to  $W = 2$  GeV. The red solid curves are the prediction of our new DCC model developed in Ref. [8]. As a comparison, we also present the prediction of our early DCC model [2, 10] (the green dotted curves), in which the amplitudes are unitary in the  $\pi N$ ,  $\eta N$ , and  $\pi\pi N(\pi\Delta, \sigma N, \rho N)$  channel space and are determined by analyzing the  $\pi N \rightarrow \pi N$  scattering up to  $W = 2$  GeV. Even without any adjustment of the model parameters to the  $\pi N \rightarrow \pi\pi N$  data, our models reproduce the available total-cross-section data to better than  $\sim 20\%$  ( $\sim 60\%$ ) accuracy at  $W < 1.6$  GeV ( $W > 1.6$  GeV). As can be seen in Fig. 2, the new DCC model has a better description of the total cross sections below  $W = 1.6$  GeV. It is noted that the multichannel unitarity including the three-body  $\pi\pi N$  channel, which gives a significant constraint on the transition probabilities between the reaction channels maintained in our model, makes it possible to have reasonable predictions for the  $\pi N \rightarrow \pi\pi N$  observables in this wide energy range from the threshold up to  $W = 2$  GeV.

In Figs. 3 and 4, we present the contribution of each partial wave to the  $\pi N \rightarrow \pi\pi N$  total cross sections. The results for partial waves up to  $J = 9/2$  are plotted. (Note that

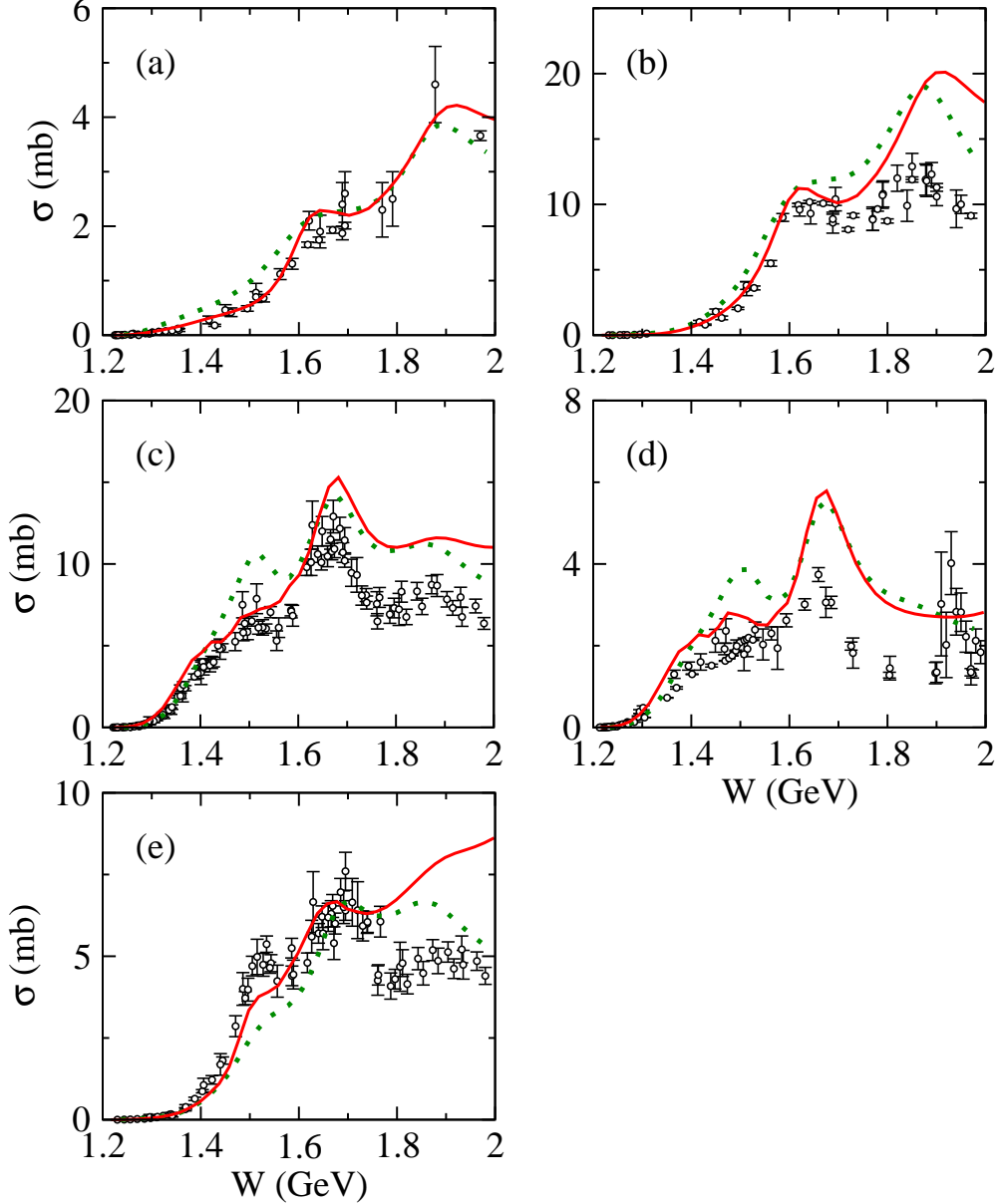


FIG. 2. (Color online) The  $\pi N \rightarrow \pi\pi N$  total cross sections predicted with the ANL-Osaka DCC models. The red solid curves are from our new model recently developed in Ref. [8], while the green dotted curves are from our early model [2]. The reaction channels are for (a)  $\pi^+p \rightarrow \pi^+\pi^+n$ , (b)  $\pi^+p \rightarrow \pi^+\pi^0n$ , (c)  $\pi^-p \rightarrow \pi^+\pi^-n$ , (d)  $\pi^-p \rightarrow \pi^0\pi^0n$ , and (e)  $\pi^-p \rightarrow \pi^-\pi^0p$ . See Refs. [1, 2] and references therein for the data.

$\pi^+p \rightarrow \pi\pi N$  contains only the isospin  $I = 3/2$  partial waves, while  $\pi^-p \rightarrow \pi\pi N$  contains both the  $I = 1/2$  and  $3/2$  partial waves.) As for the initial  $\pi^+p$  reactions, the  $F_{33}$  partial wave dominates the  $\pi^+p \rightarrow \pi^+\pi^+n$  cross section from the threshold up to  $W = 1.4$  GeV, while a couple of partial waves equally contribute to  $\pi^+p \rightarrow \pi^+\pi^0n$  at low energies. However, the  $S_{31}$  and  $D_{33}$  partial waves dominate the cross sections of both the reactions in the  $W = 1.5$ - $1.75$  GeV region; above  $W = 1.8$  GeV the  $F_{37}$  partial wave becomes dominant instead. As for the initial  $\pi^-p$  reactions, almost all the  $I = 3/2$  partial waves have only sub-dominant

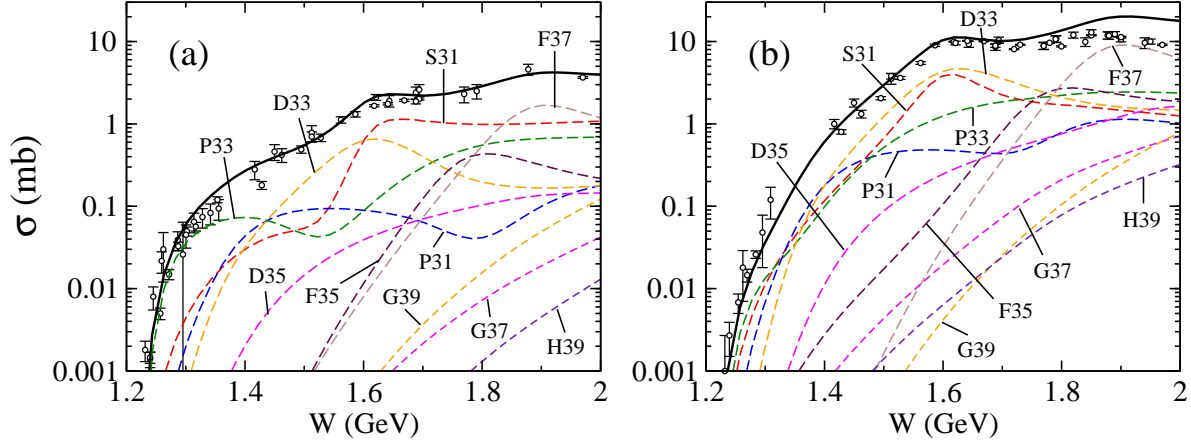


FIG. 3. (Color online) Contribution of each partial wave to the  $\pi^+p \rightarrow \pi\pi N$  total cross sections: (a)  $\pi^+p \rightarrow \pi^+\pi^+n$  and (b)  $\pi^+p \rightarrow \pi^+\pi^0p$ . The total cross section and the individual partial wave contributions are shown as thick-solid and dashed curves, respectively. See Refs. [1, 2] and references therein for the data.

contributions except for  $\pi^-p \rightarrow \pi^+\pi^-n$  and  $\pi^-p \rightarrow \pi^-\pi^0p$  at  $W \sim 1.9$  GeV where the  $F_{37}$  can be comparable to the largest  $I = 1/2$  partial waves. In the  $W$  region between 1.5 and 1.75 GeV,  $D_{13}$  and  $D_{15}$  are major partial waves for all the three charged states of the initial  $\pi^-p$  reactions, as is  $F_{15}$  for the  $\pi^+\pi^-n$  and  $\pi^0\pi^0n$  final states. It should be emphasized that the  $P_{11}$  partial wave dominates the cross sections of  $\pi^-p \rightarrow \pi^+\pi^-n$  and  $\pi^-p \rightarrow \pi^0\pi^0n$  up to  $W \sim 1.4$  GeV, where the Roper resonance exists. This is in contrast to the photoproduction reactions, for which the contribution of the Roper resonance is known to be minor on the cross sections and is obscured by the significant contribution of the first  $D_{13}$  resonance. The  $\pi N \rightarrow \pi\pi N$  reactions will thus provide crucial information not only on the high-mass  $N^*$  states, but also on the mysterious Roper resonance. The importance of the  $\pi N \rightarrow \pi\pi N$  data for the Roper resonance and the  $P_{11}$  partial wave at low energies has also been discussed with various theoretical and phenomenological approaches (see, e.g., Refs. [11–16]).

#### IV. EXAMINING POTENTIAL IMPACT OF THE $\pi N \rightarrow \pi\pi N$ DATA ON DETERMINING THE $N^*$ PARAMETERS

Now we demonstrate a potential impact of the  $\pi N \rightarrow \pi\pi N$  data on determining the  $N^*$  resonance parameters. For this purpose, we take the  $F_{37}$  partial wave as an example. As shown in Fig 3, the contribution of this partial wave is dominant for  $\pi^+p \rightarrow \pi^+\pi^+n$  and  $\pi^+p \rightarrow \pi^+\pi^0p$  above  $W = 1.8$  GeV, which is the energy region relevant to the J-PARC E45 [5] experiment. Our procedure is as follows:

1. Construct a slightly different model from that developed in Ref. [8]. For this purpose, we recall that in the DCC model of Ref. [8], each bare  $N^*$  state has the following model parameters: the bare  $N^*$  mass ( $M_{N^*}^0$ ), the cutoffs for strong and electromagnetic interactions ( $\Lambda_{N^*}$  and  $\Lambda_{N^*}^{\text{e.m.}}$ ), the coupling constants for bare  $N^* \rightarrow MB$  decays ( $C_{MB(LS),N^*}$  where the  $MB$  channel has the relative angular momentum  $L$  and the total spin  $S$ ), and the bare  $\gamma N \rightarrow N^*$  transition helicity amplitudes ( $\tilde{A}_{1/2}^{N^*}$  and  $\tilde{A}_{3/2}^{N^*}$ ). We first set the “bare” coupling constants of  $N^* \rightarrow \pi\Delta$  of the  $F_{37}$  partial wave to

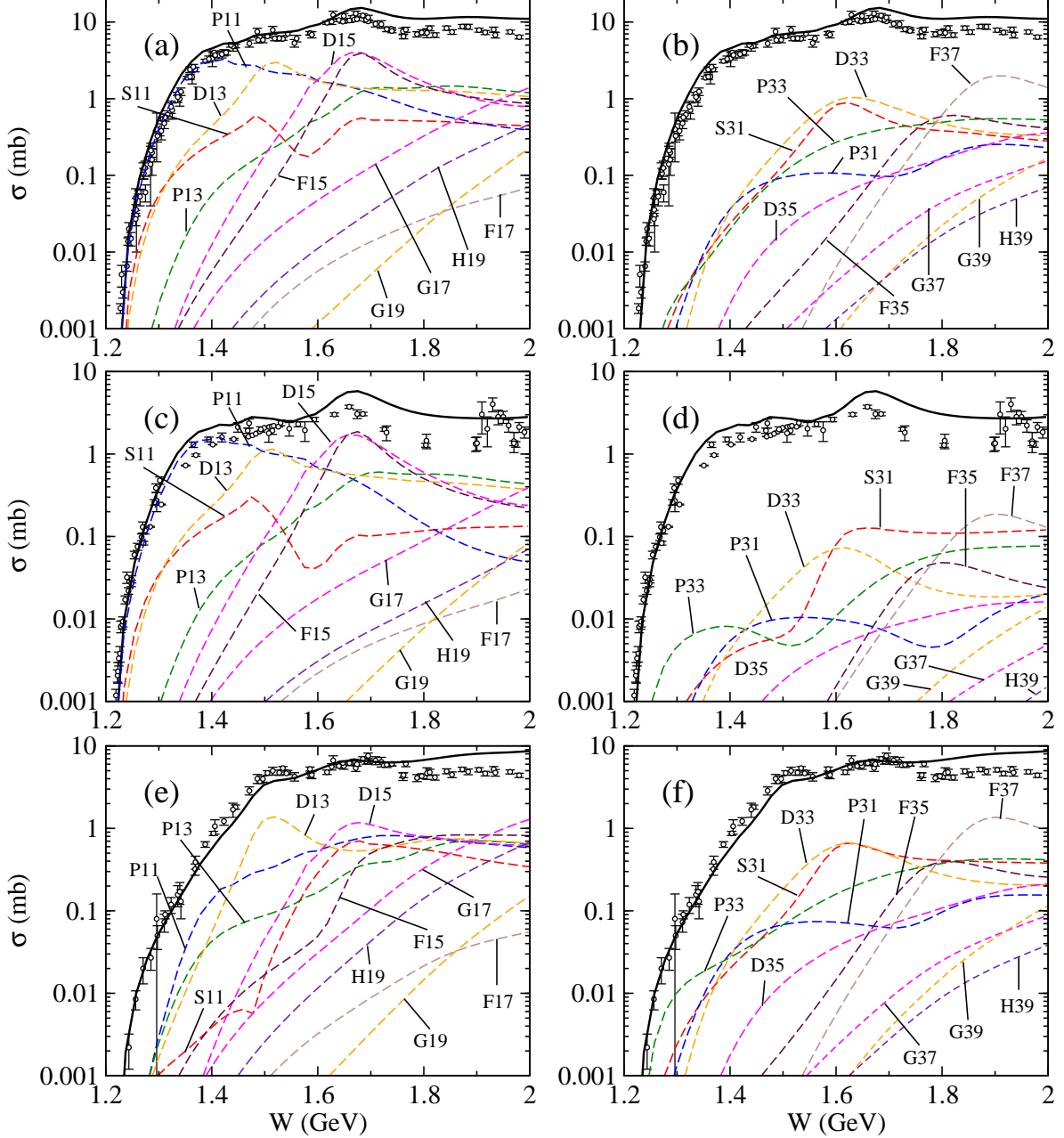


FIG. 4. (Color online) Contribution of each partial wave to the  $\pi^-p \rightarrow \pi\pi N$  total cross sections. Panels (a) and (b)  $\pi^-p \rightarrow \pi^+\pi^-n$ ; (c) and (d)  $\pi^-p \rightarrow \pi^0\pi^0n$ ; (e) and (f)  $\pi^-p \rightarrow \pi^-\pi^0p$ . Panels (a), (c), and (e) [(b), (d), and (f)] present  $I = 1/2$  [ $I = 3/2$ ] partial waves for each reaction. The total cross section and the individual partial wave contributions are shown as thick-solid and dashed curves, respectively. See Refs. [1, 2] and references therein for the data.

zero, i.e.,  $C_{MB(LS),N^*(F_{37})} = 0$  for all  $LS$  states. We then refit the  $\pi N \rightarrow \pi N, K\Sigma$  and  $\gamma N \rightarrow \pi N, K\Sigma$  data by varying only the other parameters associated with the  $F_{37}$  bare  $N^*$  states, i.e.,  $M_{N^*(F_{37})}^0$ ,  $\Lambda_{N^*(F_{37})}$ ,  $\Lambda_{N^*(F_{37})}^{\text{e.m.}}$ ,  $C_{MB(LS),N^*(F_{37})}$  with  $MB = \pi N, \rho N, K\Sigma$ ,  $\tilde{A}_{1/2}^{N^*}$ , and  $\tilde{A}_{3/2}^{N^*}$ , while all of the remaining model parameters are kept fixed as those obtained in Ref. [8]. (Note that  $F_{37}$  partial wave does not affect  $\eta N$  and  $K\Lambda$  produc-

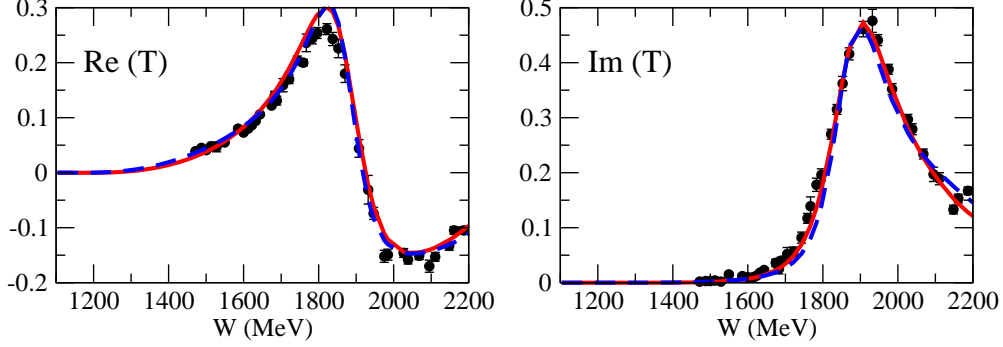


FIG. 5. (Color online)  $F_{37}$   $\pi N$  partial wave amplitude. Solid (red) curves are from the original DCC model [8]; dashed (blue) curves show the refitted DCC model. The data points are from the SAID energy-independent solution [17].

tion reactions with total isospin  $I = 1/2$  only.) Hereafter we call the DCC model of Ref. [8] the “original DCC”, while the refitted one the “refitted DCC.”

2. Examine how the difference between the original and refitted DCC emerges in the  $\pi N \rightarrow \pi\pi N$  observables.

With this exercise, we can examine whether the  $\pi N \rightarrow \pi\pi N$  data provide crucial constraints on the existing reaction models and the  $N^*$  resonance parameters that are hard to determine with the  $\pi N, \gamma N \rightarrow \pi N, \eta N, K\Lambda, K\Sigma$  data only.

In Fig. 5, we compare the  $F_{37}$   $\pi N$  partial wave amplitudes of the original and refitted DCC models. One can see that both models reproduce the  $F_{37}$  amplitudes with almost the same quality. We have also confirmed that these models give almost the same  $\chi^2$  values for the  $\pi N, \gamma N \rightarrow \pi N, K\Sigma$  data up to  $W = 2$  GeV. This result indicates that the original and refitted DCC models are hard to be distinguished from comparisons with the available data for  $\pi N, \gamma N \rightarrow \pi N, K\Sigma$  up to  $W = 2$  GeV.

For later use, we introduce the “branching ratio”  $B_{MB}$  given by

$$B_{MB} = \frac{\gamma_{MB}}{\sum_{MB} \gamma_{MB}}. \quad (6)$$

Here, the “partial decay width”  $\gamma_{MB}$  is defined for the stable meson-baryon channels ( $MB = \pi N, \eta N, K\Lambda, K\Sigma$ ) as

$$\gamma_{MB} = \rho_{MB}(\bar{k}; \bar{M}) \left| \bar{\Gamma}_{MB}^R(\bar{k}; \bar{M}) \right|^2, \quad (7)$$

where  $\rho(k; W) = \pi k E_M(k) E_B(k) / W$  with  $E_\alpha(k) \equiv \sqrt{m_\alpha^2 + k^2}$ ;  $\bar{M} = \text{Re}(M_R)$  with  $M_R$  being the complex pole mass of the  $N^*$ ; and  $\bar{k}$  is given by  $\bar{M} = E_M(\bar{k}) + E_B(\bar{k})$ . The explicit expression of the dressed  $N^* \rightarrow MB$  decay vertex  $\bar{\Gamma}_{MB}^R(k; W)$  has been given in Ref. [8] and thus will not be presented here. For the quasi-two-body channels of  $\pi\pi N$  ( $MB = \pi\Delta, \rho N, \sigma N$ ), however, the  $\gamma_{MB}$  is given as

$$\gamma_{\pi\Delta} = \frac{1}{2\pi} \int_{m_\pi + m_N}^{\bar{M} - m_\pi} dM_{\pi N} \frac{-2\text{Im}(\Sigma_{\pi\Delta}(\bar{k}; \bar{M}))}{\left| \bar{M} - E_\pi(\bar{k}) - E_\Delta(\bar{k}) - \Sigma_{\pi\Delta}(\bar{k}; \bar{M}) \right|^2} \rho_{\pi\Delta}(\bar{k}; \bar{M}) \left| \bar{\Gamma}_{\pi\Delta}^R(\bar{k}; \bar{M}) \right|^2, \quad (8)$$

for the case of  $MB = \pi\Delta$ . Here  $\Sigma_{\pi\Delta}(k; W)$  is the self-energy in the  $\pi\Delta$  Green’s function given in Ref. [8];  $\bar{k}$  is defined by  $\bar{M} = E_\pi(\bar{k}) + \sqrt{M_{\pi N}^2 + \bar{k}^2}$  for the quasi-two-body channels.



TABLE I. Comparison of pole mass ( $M_R$ ) and branching ratios ( $B_{MB}$ ) for the decay to a channel  $MB = \pi N, \pi\Delta, \rho N, K\Sigma$  of the  $F_{37}$  nucleon resonance. Allowed spin ( $S$ ) and angular momentum ( $L$ ) states for a given channel  $MB$  are listed as  $(L, S)$  in the second row.

	$M_R$ (MeV)	$B_{\pi N}$ (%)	$B_{\pi\Delta}$ (%)		$B_{\rho N}$ (%)			$B_{K\Sigma}$ (%)
		$(3, \frac{1}{2})$	$(3, \frac{3}{2})$	$(5, \frac{3}{2})$	$(3, \frac{1}{2})$	$(3, \frac{3}{2})$	$(5, \frac{3}{2})$	$(3, \frac{1}{2})$
Original DCC [8]	$1872 - i103$	51.5	46.7	0.4	1.1	0.1	0.1	0.0
Refitted DCC	$1867 - i85$	53.5	0.2	0.0	10.3	34.2	1.7	0.1

The integral in Eq. (8) accounts for the phase space of the final  $\pi\pi N$  states; Eq. (8) reduces to Eq. (7) in the stable  $\Delta$  limit:  $\Sigma_{\pi\Delta} \rightarrow 0$ . A similar expression is obtained also for  $MB = \rho N, \sigma N$ . The branching ratio defined in Eq. (6) is a good measure of relative strength of the coupling of a  $N^*$  resonance to a meson-baryon channel  $MB$  for clear resonances such as the first  $F_{37}$  resonance as shown in Fig. 5.

The resulting resonance parameters of the first  $F_{37}$  resonance are listed in Table I. We find that the original and refitted DCC models give just a slightly different pole mass:  $|M_R^{\text{orig.}} - M_R^{\text{refit}}| \sim 19$  MeV. However, the branching ratios for the decay to each component of the  $\pi\pi N$  channel ( $\pi\Delta$  and  $\rho N$ ) are significantly different between the two models, while the sum  $B_{R,\pi\Delta} + B_{R,\rho N}$  is almost the same. This suggests that a significant ambiguity may exist in their decay dynamics even for clear resonances, of which the pole mass is well determined by various analysis groups, as far as the resonance parameters are extracted from the fit without including the double pion production data.

In Figs. 6 and 7, we present the total cross sections and invariant mass distributions of  $\pi^+p \rightarrow \pi^+\pi^+n$  and  $\pi^+p \rightarrow \pi^+\pi^0p$  calculated with both the original and refitted DCC models. It is found that the two models show clear differences in those observables. As for the  $\pi^+p \rightarrow \pi^+\pi^+n$  reaction (Fig. 6), the energy dependence of the total cross section is obviously different above  $W = 1.7$  GeV, where the  $F_{37}$   $N^*$  resonance exists. As a result, the magnitude as well as the shape of the invariant mass distributions are also quite different between the two models. On the other hand, the two models give almost the same total cross sections for  $\pi^+p \rightarrow \pi^+\pi^0p$  (Fig. 7). However, the invariant mass distributions exhibit quite different shape between the two models, although the integration of the distributions gives the same total cross section. It is noticed that the peak or bump in the refitted DCC model seen at  $M_{\pi\pi} \sim 0.75$  GeV in Fig. 7(b) is more enhanced than the original DCC, while the peak at  $M_{\pi N} \sim 1.2$  GeV in Fig. 6(c) and Figs 7(c) and (d) are less enhanced. This behavior is consistent with the differences in the branching ratios between the two models shown in Table I. These differences in the predicted observables will be large enough for distinguishing the two models if the high statistics data of  $\pi N \rightarrow \pi\pi N$  at J-PARC are obtained. Also, this result indicates that the total cross sections are not enough and the differential cross section data such as the invariant mass distributions are highly desirable for a quantitative study of the  $N^*$  spectroscopy. We have confirmed that clear differences between the two models are observed also in the shape of invariant mass distributions of  $\pi^-p \rightarrow \pi^+\pi^-n$  and  $\pi^-p \rightarrow \pi^-\pi^0p$  at  $W = 1.87$  GeV, but not in  $\pi^-p \rightarrow \pi^0\pi^0n$  because of the minor contribution of  $F_{37}$  to this reaction [see Fig. 4 (c) and (d)].

Finally, we close this section with a remark about other partial waves. We have made a similar examination also for other dominant partial waves, i.e.,  $S_{31}$  and  $D_{33}$  in the initial  $\pi^+p$  reactions and  $D_{13}$ ,  $D_{15}$ , and  $F_{15}$  in the initial  $\pi^-p$  reactions. We then find that at



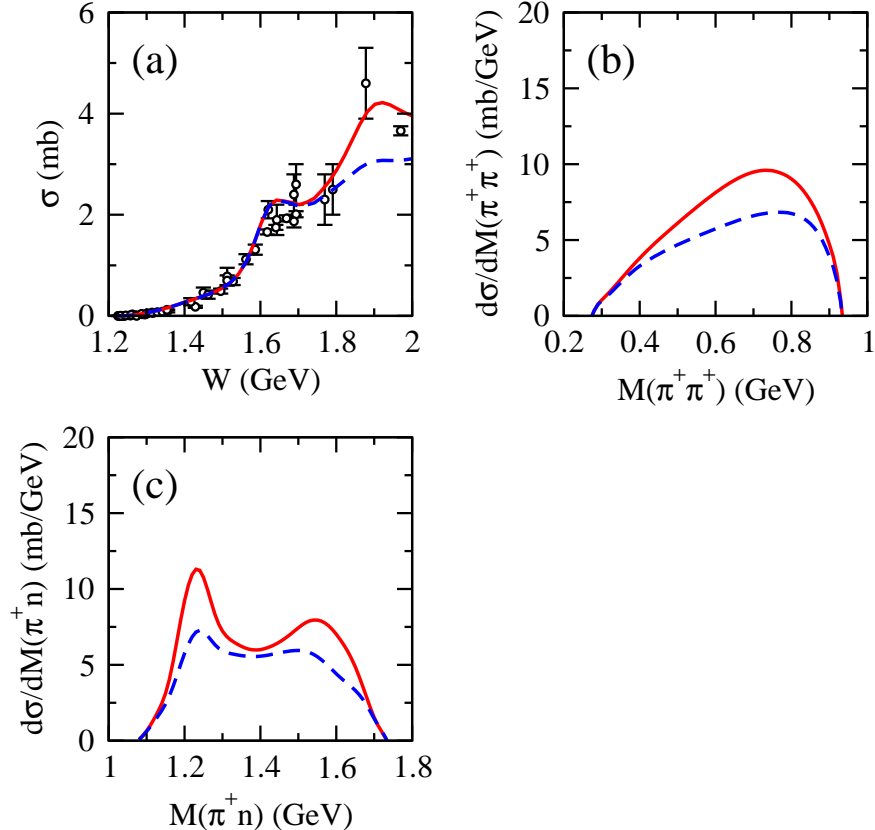


FIG. 6. (Color online) Comparison of the  $\pi^+p \rightarrow \pi^+\pi^+n$  cross sections: (a) total cross section; the invariant mass distributions of (b)  $\pi^+\pi^+$  and (c)  $\pi^+n$  at  $W = 1.87$  GeV. Solid (red) curves are the original DCC; dashed (blue) curves are the refitted DCC. See Refs. [1, 2] and references therein for the total cross section data.

least the  $N^*$  resonance parameters of  $D_{15}$  and  $F_{15}$  show uncertainties that are similar to  $F_{37}$  discussed above and could be resolved once the precise  $\pi N \rightarrow \pi\pi N$  data are available.

## V. SUMMARY AND OUTLOOK

Motivated by an experimental proposal for the measurement of the  $\pi N \rightarrow \pi\pi N$  reactions at J-PARC, we have examined a potential impact of the  $\pi N \rightarrow \pi\pi N$  data on determining the resonance parameters associated with high-mass  $N^*$  resonances, by making use of the predicted  $\pi N \rightarrow \pi\pi N$  cross sections from the ANL-Osaka DCC model recently developed in Ref. [8]. We have found that the partial wave analysis without including the double-pion production data would leave a sizable ambiguity in the  $N^*$  resonance parameters, particularly in those associated with the three-body  $\pi\pi N$  channel, and that the  $\pi N \rightarrow \pi\pi N$  data will play a crucial role for resolving the ambiguity. The results in this work clearly show that the measurement of the  $\pi N \rightarrow \pi\pi N$  reaction, such as planned at J-PARC [5], is desirable for disentangling the high-mass  $N^*$  resonances. Once the precise and extensive data of  $\pi N \rightarrow \pi\pi N$  at  $W > 1.6$  GeV are available from the proposed experiment at J-PARC, we hope to extend our combined analysis immediately and make a detailed and quantitative examination of the role of the new  $\pi N \rightarrow \pi\pi N$  data for the  $N^*$  spectroscopy. This will be

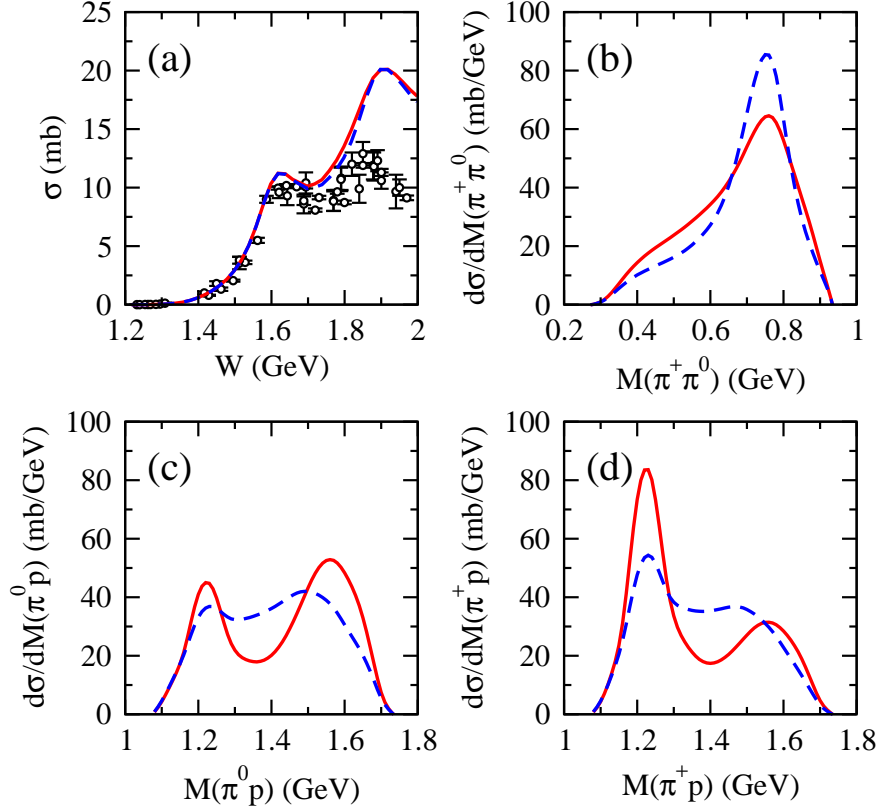


FIG. 7. (Color online) Comparison of the  $\pi^+p \rightarrow \pi^+\pi^0p$  cross sections: (a) total cross section; the invariant mass distributions of (b)  $\pi^+\pi^0$ , (c)  $\pi^0p$ , and (d)  $\pi^+p$  at  $W = 1.87$  GeV. Solid (red) curves are the original DCC; dashed (blue) curves are the refitted DCC. See Refs. [1, 2] and references therein for the total cross section data.

presented elsewhere.

## ACKNOWLEDGMENTS

The author would like to thank Dr. T.-S. H. Lee and Dr. A. M. Sandorfi for careful reading of the manuscript and helpful comments, and Dr. T. Sato for useful discussions. This work was supported by JSPS KAKENHI Grant Number 25800149. The author also acknowledges the support of the HPCI Strategic Program (Field 5 “The Origin of Matter and the Universe”) of Ministry of Education, Culture, Sports, Science and Technology (MEXT) of Japan. This work used resources of the National Energy Research Scientific Computing Center, which is supported by the Office of Science of the U.S. Department of Energy under Contract No. DE-AC02-05CH11231, and resources provided on “Fusion”, a 320-node computing cluster operated by the Laboratory Computing Resource Center at Argonne National Laboratory.

---

[1] D. M. Manley, R. A. Arndt, Y. Goradia, and V.L. Teplitz, Phys. Rev. D **30**, 904 (1984).

- [2] H. Kamano, B. Juliá-Díaz, T.-S. H. Lee, A. Matsuyama, and T. Sato, Phys. Rev. C **79**, 025206 (2009).
- [3] M. Kermani *et al.* (The CHAOS Collaboration), Phys. Rev. C **58**, 3419 (1998).
- [4] I. G. Alekseev *et al.*, Nucl. Phys. **B541**, 3 (1999).
- [5] K. Hicks and H. Sako *et al.*, Measurements of  $\pi N \rightarrow \pi\pi N$  and  $\pi N \rightarrow KY$  at J-PARC (J-PARC E45), [http://j-parc.jp/researcher/Hadron/en/pac\\_1207/pdf/P45\\_2012-3.pdf](http://j-parc.jp/researcher/Hadron/en/pac_1207/pdf/P45_2012-3.pdf).
- [6] H. Kamano, S. X. Nakamura, T.-S. H. Lee, and T. Sato, Phys. Rev. D **86**, 097503 (2012).
- [7] S. X. Nakamura, Y. Hayato, M. Hirai, H. Kamano, S. Kumano, M. Sakuda, K. Saito, and T. Sato, arXiv:1303.6032.
- [8] H. Kamano, S. X. Nakamura, T.-S. H. Lee, and T. Sato, Phys. Rev. C **88**, 035209 (2013).
- [9] A. Matsuyama, T. Sato, and T.-S. H. Lee, Phys. Rep. **439**, 193 (2007).
- [10] B. Juliá-Díaz, T.-S. H. Lee, A. Matsuyama, and T. Sato, Phys. Rev. C **76**, 065201 (2007).
- [11] A. V. Sarantsev *et al.* (CB-ELSA and A2-TAPS Collaborations), Phys. Lett. B **659**, 94 (2008).
- [12] V. Kozhevnikov and S. Sherman, Phys. Atom. Nucl. **71**, 1860 (2008).
- [13] H. Kamano and M. Arima, Phys. Rev. C **73**, 055203 (2006).
- [14] T. S. Jensen and A. F. Miranda, Phys. Rev. C **55**, 1039 (1997).
- [15] V. Bernard, N. Kaiser, and U.-G. Meißner, Nucl. Phys. **B457**, 147 (1995).
- [16] E. Oset and M. J. Vicente-Vacas, Nucl. Phys. **A446**, 584 (1985).
- [17] CNS Data Analysis Center (GWU), <http://gwdac.phys.gwu.edu>; R. Arndt, W. J. Briscoe, I. I. Strakovsky, and R. L. Workman, Phys. Rev. C **74** 045205 (2006).